3

ARRAYS

We begin with arrays of antennas before discussing particular antenna elements to show the relationship between antenna size and shape and the resulting pattern characteristics. We ignore the feed network design initially and assume that the proper array feed distribution will be obtained. At first, we assume a distribution of point sources and compute the approximate array pattern. Working with simple models provides insight rather than accuracy, and later we consider element pattern and interaction. In Chapter 12 we discuss feed network design and analysis in the discussion of phased arrays.

The chapter begins with a mathematic description of an array and gives various assumptions used to simplify the expressions. We analyze a simple two-element array to gain insight into the radiation phenomenon and how far-field patterns can be found with simple arguments. The discussion of a uniformly spaced linear array shows the Fourier series relationship between array layout and the pattern space given in sin(angle) space. The principal idea is that pattern beamwidth shrinks as the array length increases. If we space the elements too far apart, multiple beam peaks or grating lobes form in the pattern, and we show how to control these grating lobes and their relationship to maximum scan angle, array layout, and element spacing.

Phased arrays scan the beam by controlling the relative phasing between the elements. We extend the linear array to planar layouts that produce narrow beams in both principal planes. The planar array design is unchanged from the methods for linear arrays, but the grating lobe analysis shows their unique properties, as they sometimes form outside the plane of scan. We can divide the phased array into pieces to form multiple scanning beams, but the beam shape is determined by the segment size and shape used for each beam. By adding amplitude control the phased array can form multiple beams with beamwidths determined by the entire size of the array.

Each element in an array receives a portion of the power radiated by the other elements on transmittal, or scatters power into neighboring elements in reception. The

Modern Antenna Design, Second Edition, By Thomas A. Milligan

radiation from each antenna excites currents on its neighboring elements that also radiate, and we associate the total pattern with the antenna input. In an array the effective element patterns change due to this scattering. Because of reciprocity, which says that transmit and received patterns are identical, we can analyze the problem either way. This leads to mutual coupling, which we describe and analyze by mutual impedance (admittance, or scattering) matrices. This phenomenon causes the input impedance of the elements to change as we scan the array. The mutual coupling can lead to scan blindness when the feed reflection coefficient grows due to mutual coupling, and the array totally reflects the signal into the feed network. If we want the exact pattern designed for, we must compensate the feeding coefficients for the mutual coupling.

A discussion of array gain gives two methods of calculation. First, the effective area and the associated gain of a planar array cannot exceed its area when we include the extra half-element spacing area provided by the edge elements. When we space the elements so that their individual effective areas no longer overlap, array gain is the element gain multiplied by the number of elements. We can calculate gain by adding up the input power instead of integrating the pattern to compute total radiated power. We relate input power of elements to the self- and mutual resistances to determine gain of linear and planar arrays using realistic elements. The chapter ends with a discussion of three-dimensional arrays using arbitrarily oriented elements. We add this analysis to the simple array formula to handle the polarization of rotated antennas. Related to this problem is the pointing of an antenna on a positioner. We apply rotation matrices to both problems.

An array radiates or receives from two or more antennas at the same frequency. To calculate the field radiated from arrays we add the electric fields radiated from each element. The amplitudes and phases of each antenna, determined by the feed network, give us extra degrees of freedom to shape the pattern and design shifts from radiating elements to the feed network.

A single antenna radiates an electric field with both polarization components:

$$\mathbf{E} = E_\theta(\theta, \phi)\hat{\theta} + E_\phi(\theta, \phi)\hat{\phi}$$

where E_θ and E_ϕ are the two complex components (amplitude and phase) referred to some point on the antenna. If we move the antenna or the phase reference point, we only change the antenna radiated phase. We assume that the movement is small enough that the radiation approximation can still be used. Given r' as the location of the antenna relative to the phase reference point, the added phase component is $e^{j\mathbf{k}\cdot\mathbf{r}'}$, where $\mathbf{k} = 2\pi/\lambda(\sin\theta\cos\phi\hat{\mathbf{x}} + \sin\theta\sin\phi\hat{\mathbf{y}} + \cos\theta\hat{\mathbf{z}})$ and $\mathbf{r}' = x'\hat{\mathbf{x}} + y'\hat{\mathbf{y}} + z'\hat{\mathbf{z}}$ is the location of the antenna; $\mathbf{k}\cdot\mathbf{r}'$ is the phase distance from the antenna to the reference plane through the reference point and is defined by the radiation (receiving) direction. The electric field radiated from the moved antenna becomes

$$[E_\theta(\theta, \phi)\hat{\theta} + E_\phi(\theta, \phi)\hat{\phi}]e^{j\mathbf{k}\cdot\mathbf{r}'}$$

We assume that nearby objects do not alter the patterns in the movement, but we can alter element patterns if necessary.

Suppose that we have an array of antennas located at points $\mathbf{r}'_1$, $\mathbf{r}'_2$, and so on. We obtain the total pattern by adding the electric fields radiated from each:

$$\mathbf{E} = \sum_{i=1}^{N}[E_{\theta i}(\theta, \phi)\hat{\theta} + E_{\phi i}(\theta, \phi)\hat{\phi}]e^{j\mathbf{k}\cdot\mathbf{r}'_i} \tag{3-1}$$

Bringing the antennas close together will change the patterns of each because every antenna will block the radiation of the others and the distribution of currents on the elements may be changed. The shape of small resonant antennas limits the possible distribution of currents, but the magnitude and phase may be changed due to the coupling.

We make various approximations to Eq. (3-1). Changes in the patterns due to nearby antennas are ignored, and isolated element patterns are used. We assume initially a certain amplitude and phase distribution on the elements and ignore the problem of the feed network. Polarization reduces to a single term for equally polarized elements, such as dipoles, slots, or horns. If the antennas have identical element patterns, we can separate Eq. (3-1) into a product.

$$\mathbf{E} = [E_\theta(\theta, \phi)\hat{\theta} + E_\phi(\theta, \phi)\hat{\phi}] \sum E_i e^{j\mathbf{k}\cdot\mathbf{r}'_i} \tag{3-2}$$

where E_θ and E_ϕ are the normalized patterns of the single element. E_i is the electric field of the ith element, including the amplitude and phase of the feed distribution.

Equation (3-2) describes pattern multiplication that separates the pattern into an element pattern and an array factor. The method requires that all antennas have the same pattern and be orientated in the same direction. The array factor represents the pattern from an array of isotropic pattern antennas. Because array factors can be calculated by hand, we find them useful for gaining insight. We leave calculations using Eqs. (3-1) and (3-2) to the computer. The element patterns themselves could be arrays and we could use pattern multiplication to synthesize planar and volumetric arrays from linear arrays.

3-1 TWO-ELEMENT ARRAY

Consider two elements lying on the z-axis and spaced a distance d centered on the origin (Figure 3-1). If we rotate the isotropic pattern antennas around the z-axis, the problem remains unchanged, which means that all great-circle (constant ϕ) patterns are identical. On the z-axis, the element phase constant becomes $e^{jkz'\cos\theta}$. For simple line arrays we can locate pattern nulls and peaks by simple arguments.

Example Two elements are spaced $\lambda/2$ and have equal amplitudes and phases. Locate the nulls and peaks.

The phase reference planes can be placed at any convenient point. Consider the pattern at $\theta = 90^\circ$. We place the reference plane through the axis of the array. The added phase factor is zero for both elements and we just add components. The equal element phases add to give a beam peak. If we place a second reference plane through the top element, the wave radiated from the bottom element travels across the array $\lambda/2$ to the reference plane. Increasing the distance propagated decreases phase and it changes by -180°. The two out-of-phase signals cancel to produce a pattern null. The array has symmetry about the $x-y$ plane, which means that the array will have the same pattern above and below the symmetry plane. We denote this configuration an even-mode array. Figure 3-2 plots this pattern with a solid line. You should repeat the example for an odd-mode array (phases 0° and 180°) and convince yourself that the null occurs at $\theta = 90^\circ$ and the beam peak occurs at $\theta = 0^\circ$ (180°), plotted in

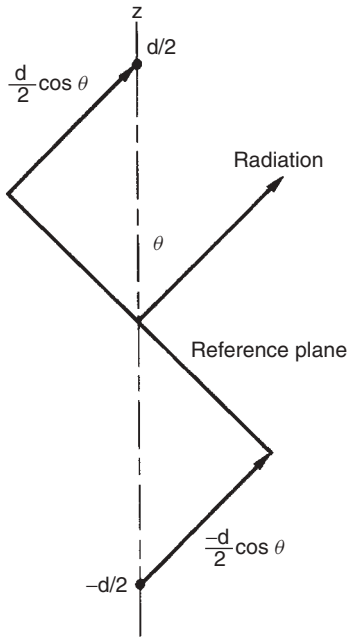

FIGURE 3-1 Two-element array on a z-axis.

Figure 3-2 as a short-dashed curve. The solid and short-dashed curves have the same directivity.

Example Suppose that the two elements are spaced $\lambda/4$, with the top element phase -90° and the bottom element phase 0°. Locate the beam peak and pattern null.

We start by placing a reference plane through the top element. The wave radiated from the bottom element travels across the array, and its phase decreases by 90°. Both radiated waves have the same phase (-90°) at the reference plane and add in phase for a beam peak. Consider a second plane through the bottom element. The wave from the top element loses 90° propagating across the array and the two waves are 180° out of phase and cancel for a null.

The second example is an end-fire array. Figure 3-2 illustrates the end-fire pattern with a long-dashed curve. All three patterns on the figure have the same directivity. The phase distribution of an end-fire array matches those of a wave traveling in the direction of the maximum. In these examples unequal amplitudes would limit the null depth to the difference. Varying the element phases while maintaining equal amplitudes changes the null directions.

Consider a general two-element array with equal amplitudes and a phase difference between them. We split the phase shift into equal parts. The top-element phase is $-\delta/2$ and the bottom-element phase is $\delta/2$. When we apply Eq. (3-2) with an isotropic element pattern, we obtain the following electric field using Euler's identity:

$$E(\theta) = 2E_0 \cos\left(\frac{\pi d}{\lambda}\cos\theta - \frac{\delta}{2}\right)\frac{e^{-jkr}}{r} \tag{3-3}$$

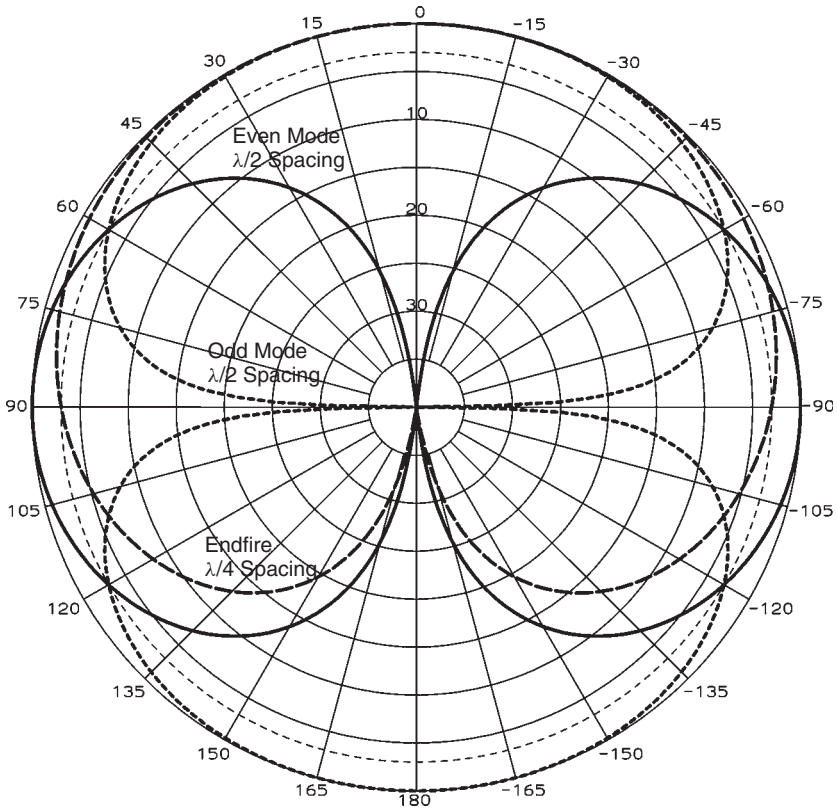

FIGURE 3-2 Two isotropic element array pattern: even-mode λ/2 spacing (solid curve); odd-mode λ/2 spacing (short-dashed curve); end-fire λ/4 spacing (long-dashed curve).

θ is measured from the z-axis. If we spaced the elements along the x-axis and found the pattern in the x–z plane, we substitute sin θ for cos θ in Eq. (3-3). In Chapter 4 we sample continuous distributions and position the elements along the x- or y-axis. Pattern peaks occur when the argument of the cosine is $n\pi$, the nulls when it is $(2n-1)\pi/2$.

$$\cos\theta_{\max} = \left(n\pi + \frac{\delta}{2}\right)\frac{\lambda}{\pi d} \tag{3-4}$$

$$\cos\theta_{\text{null}} = \left[(2n-1)\frac{\pi}{2} + \frac{\delta}{2}\right]\frac{\lambda}{\pi d} \tag{3-5}$$

If we subtract either Eq. (3-4) or (3-5) evaluated at two peaks or nulls, we get the same equation:

$$\cos\theta_1 - \cos\theta_2 = (n_1 - n_2)\frac{\lambda}{d} \tag{3-6}$$

Figure 3-3 illustrates the pattern of an equally phased two-isotropic-pattern-element array spaced 5λ along the z-axis. Because array symmetry makes the patterns on the right and left sides the same, we consider only one side. The wide element spacing

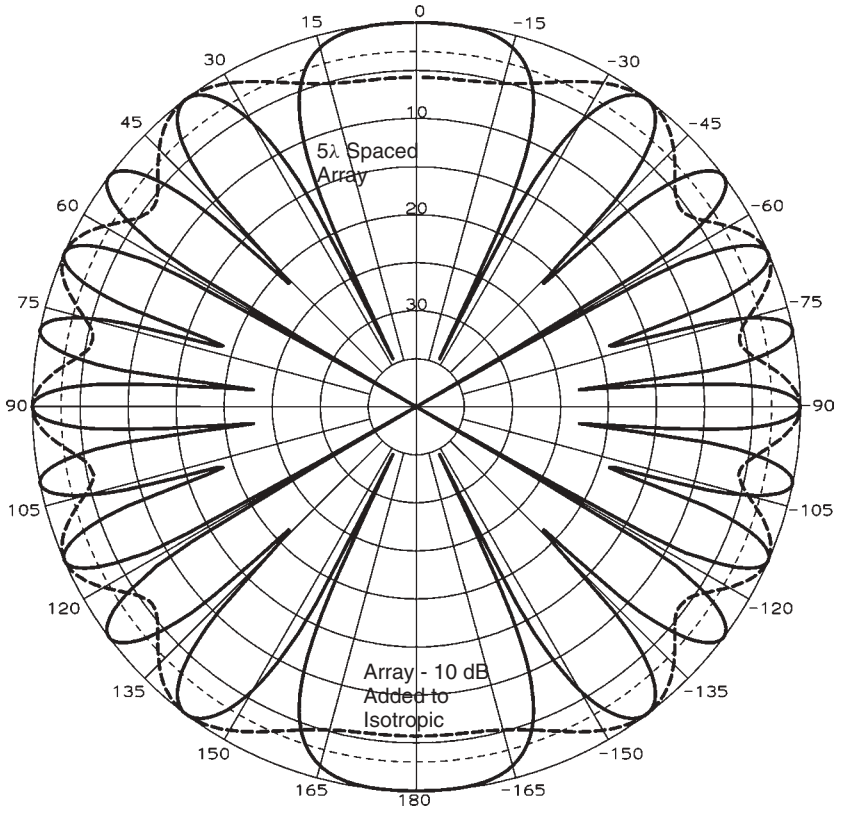

FIGURE 3-3 Two-isotropic-element array-spaced 5λ pattern (solid curve); added central element 10 dB higher power than array (dashed curve).

allows six solutions to Eq. (3-4) from 0 to 90° for the pattern peaks and five solutions for Eq. (3-5) over the same range for the nulls because the magnitude of cos θ is limited to 1. We call the multiple beams grating lobes. We usually choose the main beam and call the others grating lobes, but they are just all lobes of the array. Figure 3-3 shows that we must space the elements close together to prevent grating lobes. With a greater number of elements in the array, the amount of beam movement due to element phasing adds another factor to the prediction of when grating lobes form. The amount of phase scanning determines the maximum spacing allowed without the formation of grating lobes. The $n = 0$ lobe forms at $\theta = 90°$ and we compute the $n = 1$ mode direction from Eq. (3-4): $\theta = \cos^{-1}(\frac{1}{5}) = 78.46°$. When we substitute these angles into Eq. (3-3), we calculate a relative phase of 180° between them. The lobes have a phase of zero for n even and 180° phase for n odd in the far-field approximation. Remember we remove the exponential and $1/R$ factors from Eq. (3-3) for the far-field pattern. The actual phase of any real point depends on the distance from the center of the array.

The dashed curve in Figure 3-3 shows what happens if we add the array pattern to an isotropic radiator in the center. For a peak response of the array −10 dB relative to the isotropic antenna, we get the 5.7-dB peak-to-peak ripple shown by using Scale 1-8. The array pattern either adds or subtracts from the isotropic radiator pattern. The angular ripple rate is half that of the array lobes. Below we see that a two-element array

spaced at an integer multiple of λ/2 has a 3-dB greater gain than a single element. We feed half the power of the array into each element. By adding these factors we calculate the array element level to be −16 dB below the main central radiating antenna.

When we mount an antenna over a finite ground plane, the diffraction from the edges creates a two-element array. A 5λ-wide ground plane would produce the same pattern ripple angular rate as shown in Figure 3-3. You will often observe a similar-amplitude ripple in measured antenna patterns. Note the minimum angular distance between the peak and minimum responses in the pattern. The extra signals occur along the line in the pattern plane perpendicular to this direction. Use Eq. (3-6) to determine the distance between the array elements and you should be able to identify the structure causing the ripple. The scattering point could be on the test fixture. Consider whether the mounting structure will be different in the final configuration. You can calculate the effect from a single diffraction point by forming an array using the baseline of the primary radiator and the diffraction point. Both configurations produce the same angular ripple rate. The ripple peak occurs along that array axis, but Figure 3-3 shows that the angular ripple rate will be reduced along this end-fire direction of the $\theta = 0$ axis. If you make a careful consideration of the angular rates, in various pattern planes, you should be able to discover the cause. Always consider unexpected sources of diffraction.

You can consider the ripple using its beamwidth. To produce a symmetrical pattern about zero, we use $\sin\theta$ instead of $\cos\theta$ in Eq. (3-3), which means that the array lies along the x-axis. The −3-dB angle for the two-element uniform amplitude array can be found from Eq. (3-3):

$$\frac{\pi d}{\lambda}\sin\theta_{3\,\mathrm{dB}} = \frac{\pi}{4} \qquad \theta_{3\,\mathrm{dB}} = \sin^{-1}\frac{\lambda}{4d} \tag{3-7}$$

The beamwidth is twice Eq. (3-7). For large d we can approximate $\sin X \approx X$ and beamwidth $= \lambda/2d$. The 5λ spaced array has a beamwidth of 5.7° (0.1 rad). We can look at a 5λ-wavelength ground-plane example that has a large-amplitude element compared to the edge diffraction as two 2.5λ-spaced two-element arrays where one element has a high amplitude. Each two-element array produces a pattern with an 11.4° beamwidth the value of the composite pattern in Figure 3-3. We often mount an antenna in the center of a ground plane for measurement and observe patterns similar to Figure 3-3. If in the actual application the antenna is mounted off center, we need to add the patterns of arrays formed on both sides of the finite ground plane. The final pattern will be the composite pattern from each array and be more complicated than the simple case given above.

We calculate average radiation intensity by an integral:

$$U_{\mathrm{avg}} = \frac{4E_0^2}{\eta}\int_0^{\pi/2}\cos^2\left(\frac{\pi d}{\lambda}\cos\theta - \frac{\delta}{2}\right)\sin\theta\, d\theta$$

The directivity is

$$\frac{U_{\max}}{U_{\mathrm{avg}}} = \frac{|2E_{\max}|^2}{1 + \sin(2\pi d/\lambda)\cos\delta/(2\pi d/\lambda)} \tag{3-8}$$

where $E_{\max} = \cos[(\pi d/\lambda)\cos\theta_{\max} - \delta/2]$. When $d \geq \lambda/2$, $E_{\max} = 1$. Figure 3-4 shows the directivity versus spacing for the special cases $\delta = 0°$ and $\delta = 180°$ (even and odd modes). The directivity varies because each antenna receives power from the other. The

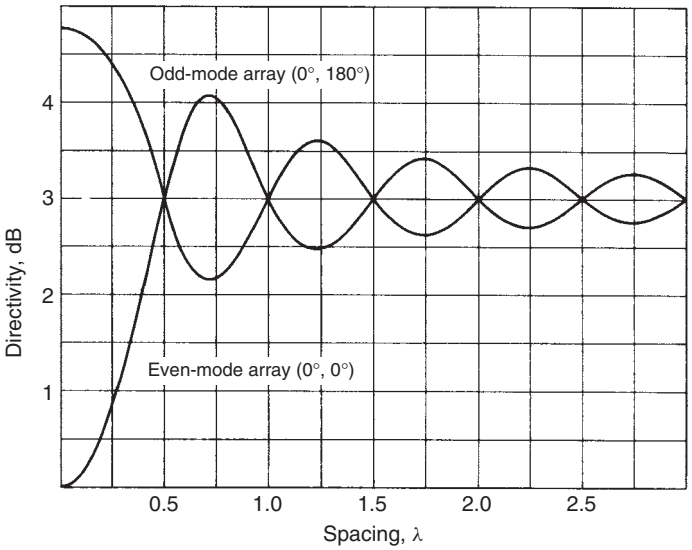

FIGURE 3-4 Directivity of even- and odd-mode two-isotropic-element arrays.

combination of the input power and the power transferred between elements changes with spacing.

3-2 LINEAR ARRAY OF N ELEMENTS

Suppose that there are N isotropic radiators equally spaced along the z-axis and fed with equal amplitudes. We assign a fixed phase shift δ between progressive elements. The array factor field is

$$\frac{\sin(N\psi/2)}{N\sin(\psi/2)} \tag{3-9}$$

where $\psi = kd\cos\theta + \delta$ [1, p. 258]. We use this to plot a universal radiation pattern for the array (Figure 3-5) for two to 10 elements. The abscissa ψ is plotted in degrees (360° is substituted for 2π in k). Both ends of the plot are lines of symmetry. The plot is periodic (period 360°). We see that the level of the first sidelobe ($N = 2$ has no sidelobe) decreases as N decreases but approaches a limit of 13.3 dB of the continuous aperture.

Figure 3-6 demonstrates the periodic pattern for $N = 6$ and shows a projection to a polar pattern when the progressive phase between elements is zero and the elements are spaced $\lambda/2$. We can plot similar curves for other array distributions; all have a period of 360°. Figure 3-6 illustrates the use of a circle diagram, a method of constructing a polar pattern from the universal pattern such as Eq. (3-9) for the uniform-amplitude distribution. An array can be analyzed as a sampling of the continuous distribution that produces a Fourier series of the distribution. A Fourier series has multiple responses. In Chapter 4 we design large arrays by sampling continuous distributions. The pattern angle of an array is measured either from the axis using cosine of pattern angle or is measured broadside using sine. You should become comfortable with either notation since the sine and cosine of angles involves only a complementary operation of the angles.

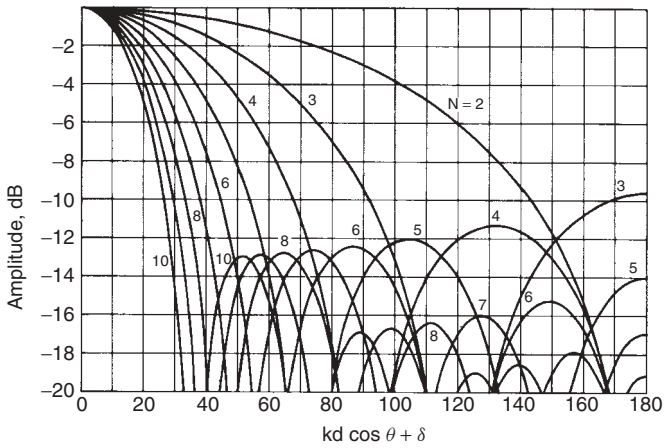

FIGURE 3-5 ψ-space pattern of linear arrays with a uniform amplitude distribution.

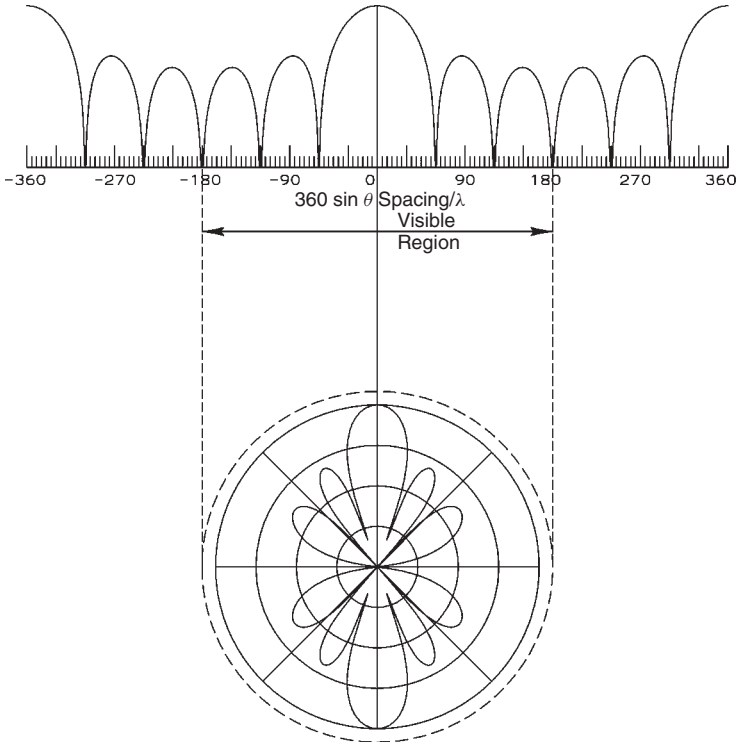

FIGURE 3-6 Circle diagram of a six-element uniform-amplitude array with λ/2 spacing.

Since $\cos\theta$ (or $\sin\theta$) is limited to ± 1, the region along the abscissa of the universal pattern used (the visible region) is found from the range of ψ:

$$\frac{-360^\circ d}{\lambda} + \delta \quad \text{to} \quad \frac{360^\circ d}{\lambda} + \delta$$

The circle diagram is constructed by first drawing a circle the same diameter as the visible region below the universal diagram centered at δ, the progressive phase shift between elements. Figure 3-6 has a $\delta = 0$. Since the element spacing is $\lambda/2$, the range is $\pm 180^\circ$. The polar pattern radius equals the amplitude of the universal pattern. Both the universal pattern and the polar pattern use a logarithmic (dB) scale from 0 to -40 dB. Projecting points vertically from the universal pattern to the visible region performs the cosine or sine operation, and the polar pattern becomes the real pattern in space. We project each point vertically until it intersects the dashed visible region circle in two places and then draw lines from these points to the center. After you project the nulls and peaks of the universal pattern to the dashed circle, it is easy to sketch the polar pattern. The circle diagram helps us visualize patterns and the effects of scanning, but no one would do serious design with it. Second, it is useful only for small arrays because large arrays produce unwieldy diagrams.

When the spacing between elements is greater than $\lambda/2$, the visible region widens to include more than one periodic main lobe and the array has multiple beams. To have a beam centered at θ_1, set the progressive phase difference between elements:

$$\delta = \frac{-360^\circ d}{\lambda} \cos \theta_1 \tag{3-10}$$

End fire ($\theta_1 = 0$) occurs when

$$\delta = \frac{-360^\circ d}{\lambda} \tag{3-11}$$

We can use Figure 3-5 to compute beamwidth angles of arrays. Table 3-1 is a list of the ψ-space angles of the 3- and 10-dB levels.

Example A six-element equally spaced uniform array has spacings of $\lambda/2$ and zero progressive phase shift between elements ($\delta = 0^\circ$). Calculate the 3-dB beamwidth.

We read from Table 3-1 the value $\psi_{3\,\text{dB}} = 26.90^\circ$. Because the pattern is symmetrical in ψ space (Figure 3-6), the second $\psi_{3\,\text{dB}}$ is -26.9°.

$$kd \cos \theta_{1,2} + \delta = \pm \psi_{3\,\text{dB}}$$

$$\frac{360^\circ}{\lambda} \frac{\lambda}{2} \cos \theta_{1,2} = \pm 26.90^\circ \qquad \cos \theta_{1,2} = \frac{\pm 26.9^\circ}{180^\circ}$$

$$\theta_1 = 81.4^\circ \qquad \theta_2 = 98.6^\circ$$

TABLE 3-1 ψ-Space Angles of 3- and 10-dB Levels of an Equal-Amplitude Distribution Array (deg)

N	3 dB	10 dB	N	3 dB	10 dB	N	3 dB	10 dB
2	90.00	143.13	11	14.55	24.21	20	7.980	13.29
3	55.90	91.47	12	13.33	22.18	24	6.649	11.08
4	40.98	67.63	13	12.30	20.47	28	5.698	9.492
5	32.46	53.75	14	11.42	19.00	32	4.985	8.305
6	26.90	44.63	15	10.65	17.74	36	4.431	7.382
7	22.98	38.18	16	9.98	16.62	40	3.988	6.643
8	20.07	33.36	17	9.39	15.64	50	3.190	5.314
9	17.81	29.62	18	8.87	14.77	64	2.492	4.152
10	16.02	26.64	19	8.40	14.00	100	1.595	2.657

Remember that θ is measured from the axis of the array (z-axis) and the 3-dB beamwidth is the difference (17.2°). On Figure 3-6 the visible region ranges between $-180°$ and $+180°$. There are four sidelobes in the visible region (Figure 3-6). Since an array samples a continuous aperture distribution, the continuous distribution is Nd long. We can estimate beamwidth by using a uniform amplitude distribution:

$$\text{HPBW} = 50.76° \frac{\lambda}{Nd} = 16.92°$$

This formula approximates the array beamwidth reasonably.

Example A six-element array has a progressive phase shift δ of 90° between elements. Compute the 10-dB beam edge angles for $\lambda/2$ spacing.

Figure 3-7 shows the circle diagram analysis of this example. The line to the center of the polar pattern has been shifted to 90° and the pattern spans 360° of the linear scale. By projecting the nulls and peaks to the circle below, the pattern can easily be sketched.

$$\psi_{10\,\text{dB}} = \pm 44.63° \quad \text{(Table 3-1)}$$
$$kd \cos\theta_{1,2} = \pm\psi_{10\,\text{dB}} - \delta$$

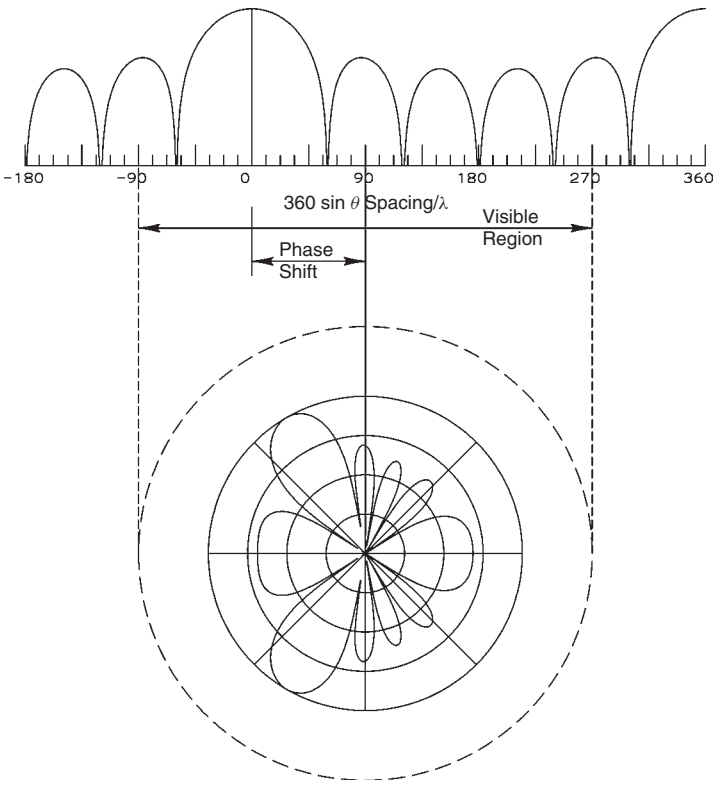

FIGURE 3-7 Six-element uniform-amplitude array with $\lambda/2$ spacing scanned with 90° progressive phase shift between elements.

Solving for $\cos\theta_{1,2}$, we have

$$\cos\theta_{1,2} = \frac{\pm\psi_{10\,\mathrm{dB}} - \delta}{kd} = \frac{\pm 44.63^\circ - 90^\circ}{180^\circ}$$

$$\theta_1 = 104.6^\circ \qquad \theta_2 = 138.4^\circ \qquad \text{beamwidth} = 33.8^\circ$$

There are five sidelobes in the visible region (Figure 3-7). Equation (3-9) gives the beam maximum direction:

$$\cos\theta_0 = \frac{-\delta}{kd} = \frac{-90^\circ}{180^\circ} \qquad \theta_0 = 120^\circ$$

The main beam is no longer symmetrical about the beam peak. The 3-dB pattern angles are 110.5° and 130.5°. The beamwidth (3-dB beamwidth = 20°) increases with scan angle. What element spacing would result in this beamwidth for broadside radiation ($\delta = 0^\circ$)?

$$\frac{360^\circ}{\lambda} d\cos\theta_1 = 26.90^\circ \quad \text{(Table 3-1)}$$

On solving for spacing, we have

$$\frac{d}{\lambda} = \frac{26.9^\circ}{360^\circ\cos\theta_1}$$

Remember that the beam is centered on $\theta = 90^\circ$, so that $\theta_1 = 90 - 20/2 = 80^\circ$.

$$\frac{d}{\lambda} = \frac{26.9^\circ}{360^\circ\cos 80^\circ} = 0.431$$

The effective spacing has been reduced by approximately the cosine of the scan angle from $\theta = 90^\circ$, broadside:

$$\frac{d}{\lambda}\cos 30^\circ = 0.433$$

The accuracy of the cosine relation increases with more elements.

Example Determine the progressive phase shift between elements for an end-fire array with 0.3λ element spacing and compute beamwidth for a uniform distribution array with five elements.

Figure 3-8 illustrates this example using the circle diagram. End fire occurs when [Eq. (3-11)]

$$\delta = \frac{-360^\circ(0.3\lambda)}{\lambda} = -108^\circ$$

This is the progressive phase shift for all distributions with 0.3λ element spacing for an end-fire pattern. Table 3-1 gives the ψ-space angle, $\psi_{3\,\mathrm{dB}} = \pm 32.46^\circ$. Substituting in the expression for ψ, we have

$$\frac{360^\circ(0.3\lambda)}{\lambda}\cos\theta_{1,2} = \pm 32.46^\circ$$

$$\cos\theta_{1,2} = \frac{\pm 32.46^\circ + 108^\circ}{360^\circ(0.3)}$$

$$\cos\theta_1 = \frac{140.46}{108} = 1.301 \qquad \cos\theta_2 = \frac{75.46}{108} = 0.699$$

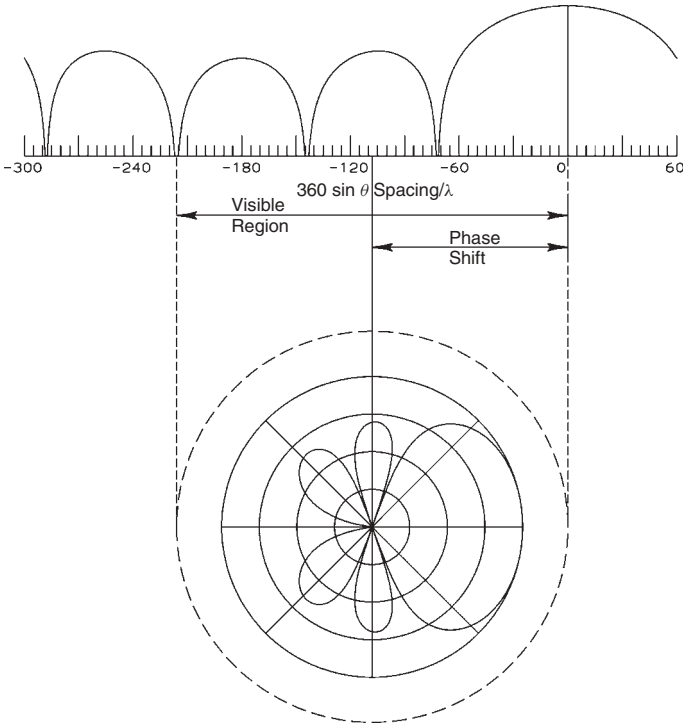

FIGURE 3-8 Five-element uniform-amplitude array scanned to end fire.

θ_1 is in invisible space, since $|\cos\theta| \leq 1$; $\theta_2 = 45.6^\circ$. Symmetry about the z-axis supplies us with the second angle $\theta_1 = -45.6^\circ$ and beamwidth is the difference: 91.2°. The end-fire array samples a traveling-wave distribution. The continuous uniform distribution phased for end fire with the same length has a 90.4° beamwidth.

Remember that we have been dealing with isotropic pattern antennas. For example, broadcast towers, seen from above, approximate isotropic antennas in the horizontal plane. The patterns of the individual antennas modify the results of isotropic antenna arrays. In small arrays the element pattern is quite significant, but the beamwidths of large arrays are determined mainly by the array factor. The beamwidths calculated for array factors approximate the actual beamwidths only when the elements have significant patterns. We must rely on computer solutions of specific cases, including the element pattern, for better results.

3-3 HANSEN AND WOODYARD END-FIRE ARRAY [2]

The end-fire array directivity increases if the sum of the progressive phase shifts between elements is decreased by approximately π. The equivalent traveling-wave velocity slows in the structure relative to free space. The progressive phase shift between elements becomes

$$\delta = -kd - \frac{2.94}{N} \simeq -kd - \frac{\pi}{N} \qquad \text{rad} \tag{3-12}$$

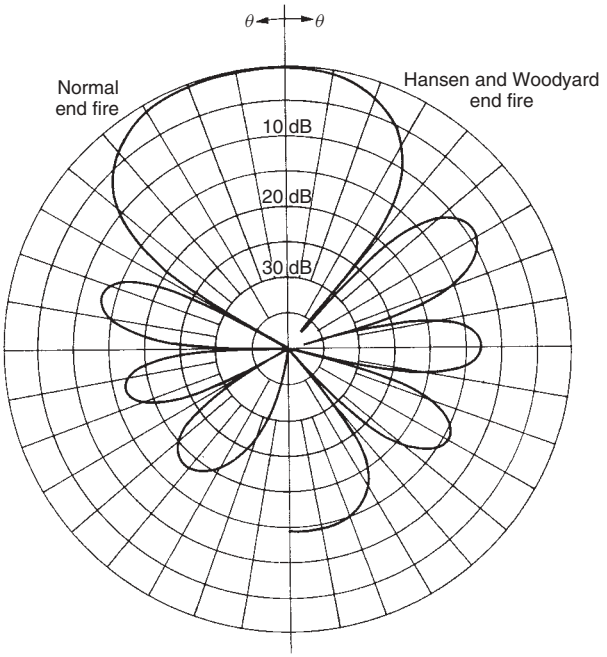

FIGURE 3-9 Patterns of a normal end fire and a Hansen and Woodyard end-fire array of isotropic elements.

where N is the number of elements in the array. The normal end-fire progressive phase shift between elements, $\delta = -kd$, places one edge of the visible region at the origin of ψ space. This method shifts the edge to a lower portion of the curve. The universal radiation curve peak (Figure 3-5) shifts into invisible space and the sidelobes rise in proportion to the new beam peak, but the beamwidth narrows. Equation (3-12) holds strictly only for large arrays, but the directivity increases for all arrays when it is applied.

Example Suppose that eight elements are spaced $\lambda/4$ apart with a uniform amplitude distribution. Compare the two endfire designs. The two patterns are compared in Figure 3-9.

The results are as follows: The beamwidth decreases, and the directivity increases by 2.5 dB. The sidelobes rise to 9 dB from 13 dB.

3-4 PHASED ARRAYS

Suppose that a wave approaches at an angle to the axis of an array located on the z axis (Figure 3-10). The wave reaches the top element first and progresses down the array in succession. If the signals are added directly, they will cancel each other to some extent because they have a progression of phases. Figure 3-10 shows the results of adding a series of time delays to equalize the path lengths in the lines where the position z_i along the axis determines the time delay τ_i for incident angle θ_0:

$$\tau_i = \frac{z_i}{c} \cos \theta_0 + \tau_0$$

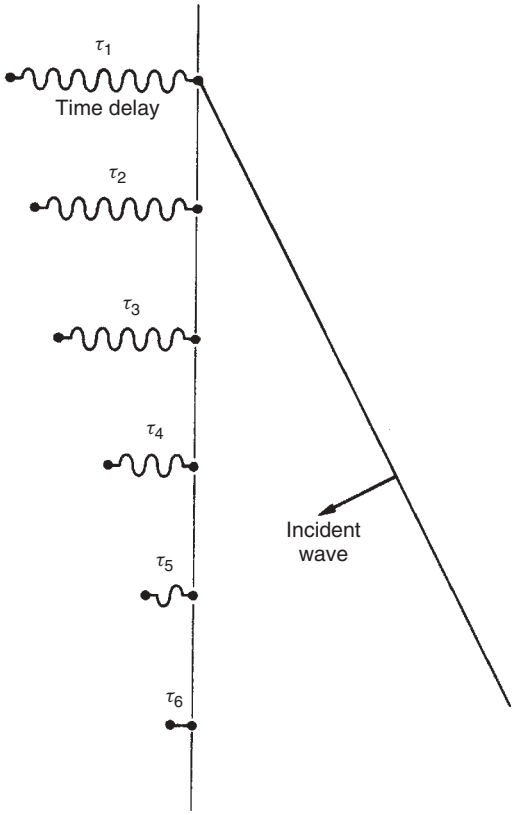

FIGURE 3-10 Linear array scanned with time-delay networks.

and velocity of light c. We add an arbitrary time delay τ_0 to keep all time delays, τ_i, positive. This feed network is frequency independent, as we vary the progression of time delays to scan the beam.

Phase shifters replace the time-delay networks in phased arrays. They provide equivalent beam scanning at a single frequency. To scan to an angle θ_0, the required phase shift is

$$-\frac{2\pi}{\lambda} z \cos\theta_0 \quad \text{modulo } 2\pi \quad \text{(rad)}$$

$$\frac{-360^\circ}{\lambda} z \cos\theta_0 \quad \text{modulo } 360^\circ \quad \text{(deg)}$$

for elements located on the z-axis. For a general space array we must counteract the phase difference to the reference plane, $e^{j\mathbf{k}\cdot\mathbf{r}'}$, for the direction of scan so that the phases of all elements are zero. To scan in the direction (θ_0, ϕ_0), we must add a phase factor to every element, depending on its position. The phase factor on each element of a general space array is

$$e^{-j\mathbf{k}_0 \cdot \mathbf{r}'} \tag{3-13}$$

where

$$\mathbf{k}_0 = \frac{2\pi}{\lambda}(\sin\theta_0 \cos\phi_0 \hat{\mathbf{x}} + \sin\theta_0 \sin\phi_0 \hat{\mathbf{y}} + \cos\theta_0 \hat{\mathbf{z}})$$

is the vector propagation constant in the direction of the beam and **r** is the element location. Adding this phase factor to the element phases causes the product of the exponential factors [Eq. (3-2)] to be 1 at the scan angle, and the components E_i add in the scan direction.

Using phase shifters limits the frequency bandwidth. Given a fixed phase shift over a small frequency range, increasing the frequency scans the beam toward broadside:

$$\Delta\theta = \frac{f_2 - f_1}{f_2} \tan\left(\frac{\pi}{2} - \theta_0\right) \qquad \text{rad} \tag{3-14}$$

where θ_0 is the scan angle [3]. Limiting the allowable scanning with frequency to plus or minus one-fourth of the local beamwidth defines the bandwidth of the array. When the beam is scanned to 30° off the axis, the bandwidth is related directly to the beamwidth at broadside ($\theta = 90°$):

$$\text{bandwidth}(\%) \simeq \text{beamwidth (deg) at } \theta_0 = 30^\circ$$

The beam shifts less with frequency near broadside, since the tangent factor in Eq. (3-14) approaches zero. A general estimate is given by

$$\text{bandwidth}(\%) \simeq \frac{\text{beamwidth (deg)}}{2\cos\theta_0} \tag{3-15}$$

where the broadside beamwidth is used.

Example Given an array with 100 elements spaced at λ/2, determine the bandwidth when scanned to 45°.

The beamwidth is estimated from the aperture width:

$$\text{HPBW} = \frac{50.76^\circ}{100(\frac{1}{2})} \simeq 1^\circ$$

$$\text{bandwidth}(\%) \simeq \frac{1}{2\cos 45^\circ} = 0.7\%$$

Any radar antenna would have a broader beamwidth because the sidelobes need to be reduced, but this is a good first estimate.

The bandwidth can be increased by feeding subarrays with time-delay networks. The subarrays continue to be scanned with phase shifters. Only a few time-delay networks are needed, and the subarray beamwidth determines the bandwidth. In Chapter 12 we discuss the problems caused by using subarrays.

3-5 GRATING LOBES

Phased arrays vary the progressive phase by Eq. (3-13) to scan the beam. When the array element spacing is greater than λ/2, the appearance of secondary beam peaks (grating lobes) limits the scan angle. The grating lobe attains full amplitude when

$$\frac{d}{\lambda}(1 + \cos\theta_{\text{gr}}) = 1 \qquad \theta_{\text{gr}} = \cos^{-1}\left(\frac{\lambda}{d} - 1\right) \tag{3-16}$$

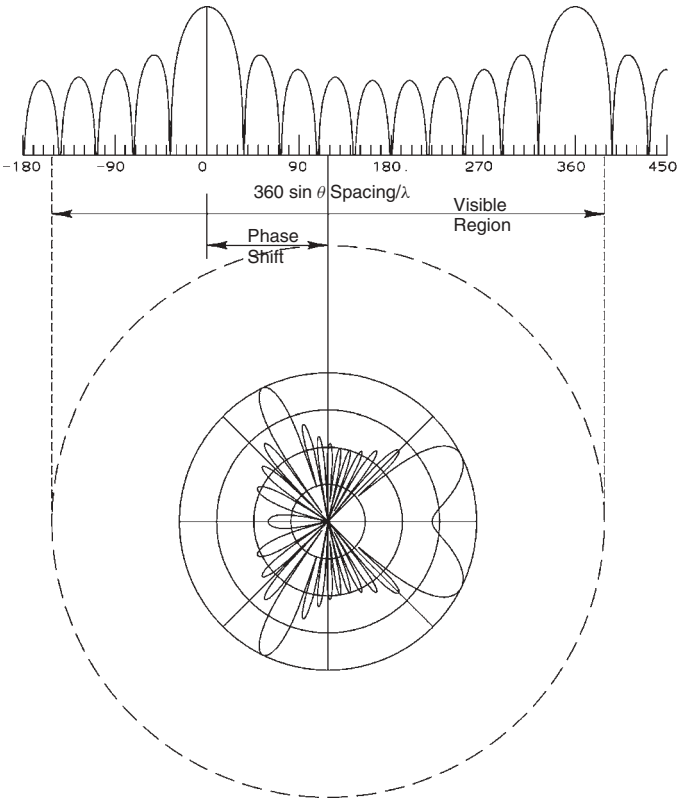

FIGURE 3-11 Ten-element array with 3λ/4 spacing scanned to 26°, showing the onset of a grating lobe.

Example The spacing of the elements of an array is 0.75λ. Determine the scan angle when the grating lobe is full amplitude.

$$\theta_{gr} = \cos^{-1}\left(\frac{4}{3} - 1\right) = 70.5^\circ$$

At this point the grating lobe is the same amplitude as the main beam. The lobe does not appear suddenly, but it grows as the visible region shifts and starts including the second periodic main lobe. Figure 3-11 shows the grating lobe formation for an array with 0.75λ element spacings on a circle diagram. The dashed circle of the visible region spans more than one beam of the universal radiation pattern of the uniform amplitude array.

Arrays with element spacing greater than λ always have grating lobes (multiple main beams), but the pattern of the antenna elements may reduce the grating lobes to acceptable levels and allow a wide element spacing.

3-6 MULTIPLE BEAMS

An array can form multiple beams. Equation (3-13) gives the phase coefficients to multiply each element feed voltage E_i to scan it to a given angle. The array will form

a second beam if we add a second distribution: $E_i e^{-j\mathbf{k}_2\cdot\mathbf{r}'_i}$. The distribution E_i remains constant for both beams. We add the two distributions to obtain both beams:

$$E_i(e^{-j\mathbf{k}_1\cdot\mathbf{r}'_i} + e^{-j\mathbf{k}_2\cdot\mathbf{r}'_i}) \tag{3-17}$$

This multiplies the distribution E_i by a second distribution whose amplitudes and phases are functions of the antenna position and the scan angles of the two beams. Each beam uses the entire array to form its beam. In a phased array both phase and amplitude must be varied to achieve multiple beams. An array, which can only vary phase, must be divided into subarrays to form multiple beams, but its beamwidths will depend on the subarray widths.

We can produce unequal beams with different amplitude distributions and pattern shapes if needed. We can add as many beams as necessary by including the distribution element factors with the scanning phase coefficients in Eq. (3-17). The element feeding coefficients become the sum.

Example Compute the feed coefficients of a 15-element array with $\lambda/2$ spacings and a uniform distribution scanned to 45° and 120° from the z-axis.

First center the array on the z-axis. The elements are located at

$$z_i = \frac{(-8+i)\lambda}{2}$$

To scan to 45°, the element phase factors are

$$\exp(-jkz_i\cos 45^\circ) = \exp\left[-j\frac{360^\circ}{\lambda}\frac{1}{\sqrt{2}}\frac{(-8+i)\lambda}{2}\right]$$

To scan to 120°, the element phase factors are $e^{j90^\circ(-8+i)}$. The ninth-element ($z_9 = \lambda/2$) phase factors are $e^{-j127.3^\circ}$ and e^{j90°. Assume a voltage magnitude of one-half for each uniform-amplitude-distribution beam so that the center element has a magnitude of 1. We sum the distributions to calculate the feeding coefficient of the ninth element:$0.32e^{j161.4^\circ}$. When converted to decibel ratios, Table 3-2 lists the feeding coefficients for the array. We can estimate both beamwidths from Table 3-1. $\psi_{3\,\mathrm{dB}} = 10.65^\circ$:

$$\cos\theta_{1,2} = \begin{cases} \dfrac{\pm 10.65^\circ + 127.28^\circ}{180^\circ} & \theta_1 = 40^\circ, \theta_2 = 49.6^\circ \\ \dfrac{\pm 10.65^\circ - 90^\circ}{180^\circ} & \theta_1 = 116.2^\circ, \theta_2 = 124^\circ \end{cases}$$

The pattern (Figure 3-12) has these beams.

The gain of each beam depends on the feed network. If a single input supplies power to two beams, each beam can receive only half the input power and gain reduced 3 dB for both beams. Butler matrices [4] and Blass beamforming networks [5] supply an input for each beam. The inputs are isolated from each other and the transmitter power in each port feeds only one beam, and therefore the full array gain is available to each input. Similarly, we can place a receiver on each port and use the full effective area for each.

TABLE 3-2 Feeding Coefficients for a Dual-Beam 15-Element Array

Element	Beamwidth (dB)	Angle (deg)	Element	Beamwidth (dB)	Angle (deg)
1	−2.38	130.48	9	−9.91	161.36
2	−8.59	111.84	10	−1.99	142.72
3	−0.01	−86.80	11	−1.64	−55.92
4	−11.49	74.56	12	−11.49	−74.56
5	−1.64	55.92	13	−0.01	86.80
6	−1.99	−142.72	14	−8.59	−111.84
7	−9.91	161.36	15	−2.38	−130.48
8	0.00	0.0			

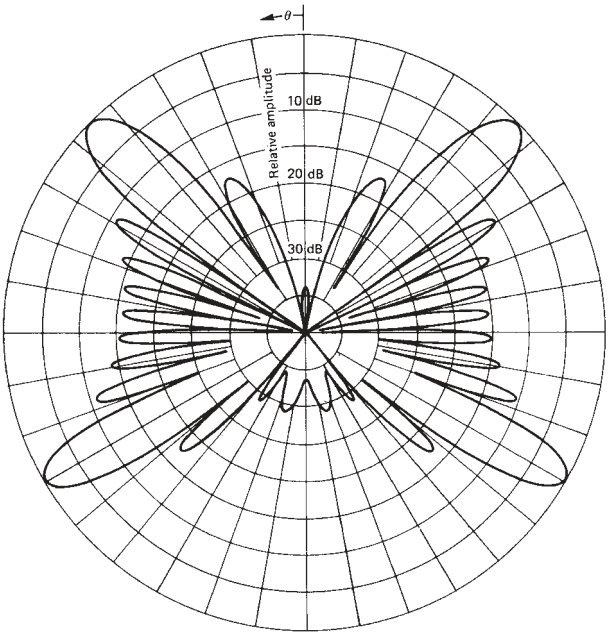

FIGURE 3-12 Fifteen-element linear array pattern with simultaneous beams at $\theta = 45^\circ$ and 120°.

We will delay the important topics of array synthesis and sidelobe reduction until after we have discussed aperture distributions. A trade-off is made between the beamwidth and the sidelobe levels. The beamwidth narrows only by putting more power into the sidelobes.

3-7 PLANAR ARRAY

The linear array only controls the pattern in one plane; it depends on the element pattern to control the beam in the other plane. Planar arrays can control the beam shape in both planes and form pencil beams. Whereas a linear array can only scan in

a single plane, a planar array can scan to any angle in the upper hemisphere. Most planar arrays rely on the element pattern or ground plane to eliminate the backlobe on the opposite side of the plane. The planar array has $N - 1$ nulls that can be used to control the pattern where N is the total number of elements.

A simple feed distribution uses the product of two linear arrays. This eliminates many degrees of freedom of the array because an $M \times N$ array would be determined by $M - 1 + N - 1$ nulls when we could have used $M \times N - 1$ possible nulls. Figure 3-13 shows the spherical pattern of a uniformly spaced 8×8 planar array where all elements are fed the same amplitude where a 90° beamwidth element eliminates the backlobe. The pattern along either principal axis shows the steady sidelobe reduction that starts with -13.2 dB. Diagonal plane sidelobes are the product of the sidelobes in the principal planes. The first sidelobe in the diagonal plane is down 26.4 dB. An array feed distribution, not a product of two linear arrays, can yield more equal sidelobes in all pattern planes.

Figure 3-14 illustrates the pattern of the rectangular array when the element feeding coefficients are phased to scan the beam along one principal plane. The main beam broadens in the plane of scan as the effective array length is reduced but stays narrow in the orthogonal plane. More sidelobes appear behind the main beam. We see a large sidelobe growing on the horizon that will become a grating lobe when the array is scanned further. The sidelobes in the plane orthogonal to the plane of scan move with the main beam but roll into a cone that becomes tighter with increased scan.

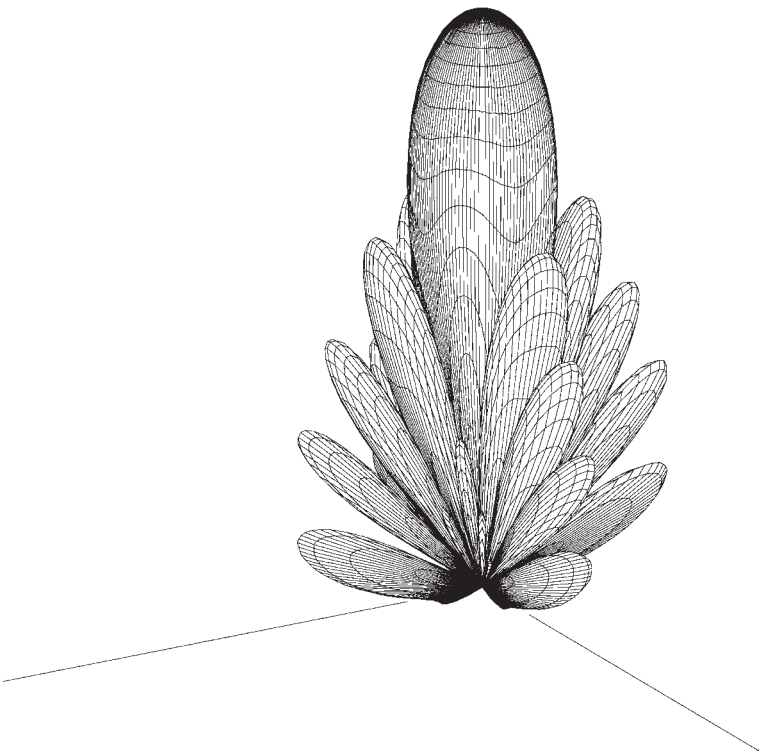

FIGURE 3-13 Spherical radiation pattern of an 8×8-element uniform-amplitude and spaced square planar array.

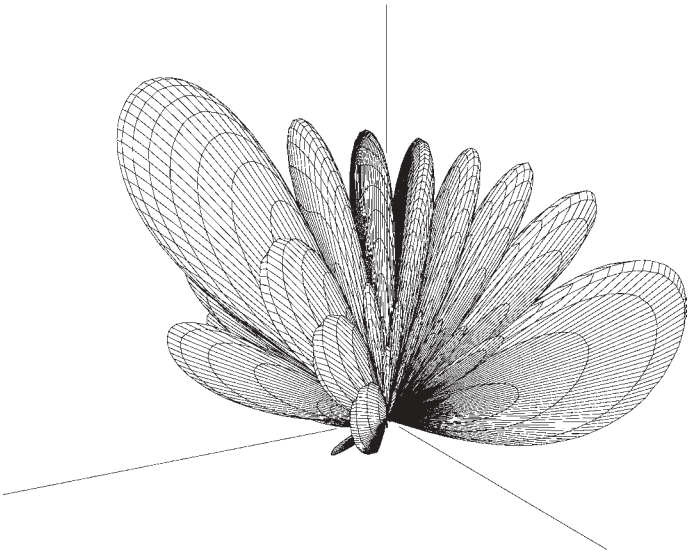

FIGURE 3-14 Spherical radiation pattern of an 8 × 8-element square-planar array scanned along a principal plane.

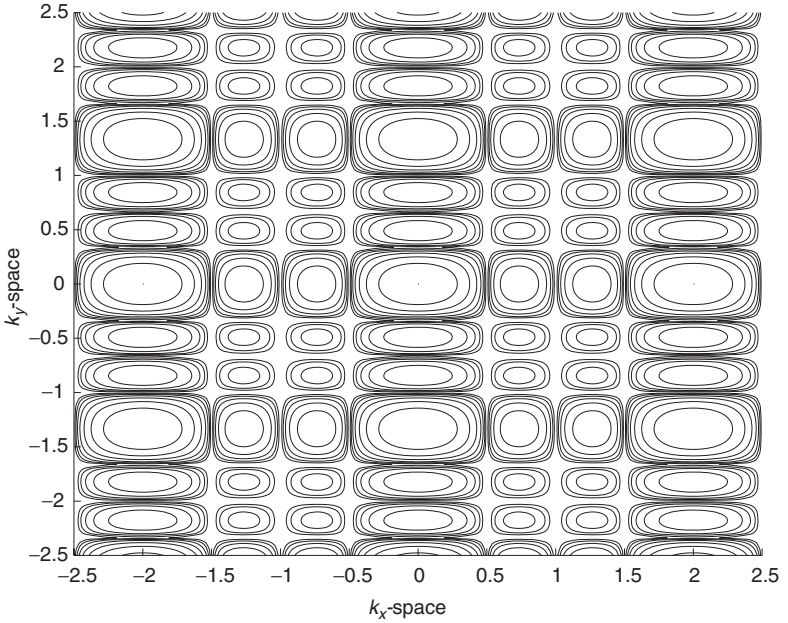

FIGURE 3-15 Contour plot of the pattern of a 4 × 4-element square array in $k_x k_y$-space showing multiple beams and sidelobes.

Figure 3-15 shows a contour plot of the universal pattern of a 4 × 4 element rectangular array. We denote this universal pattern $k_x k_y$ space because the principal axes have sin θ factors similar to the universal pattern of a linear array. The array for Figure 3-15 has its y-axis element spacing 1.5 times wider than the x-axis spacing. The diagram axes extend until multiple beams show on the figure. The main beams correspond

to the center of the large "squares." The visible region on the figure is a unit circle with its center at the negative scan direction $(-k_{x0}, -k_{y0})$. This technique mirrors the circle diagram of the linear array where the visible region is given by a linear region centered at the negative scan direction. You should notice that the diagonal sidelobes have smaller amplitudes than the principal plane sidelobes. We move the unit circle as the array scans and the diagram shows those locations of scan that have multiple beams (grating lobes). A grating analysis simplifies the diagram of Figure 3-15 to the main beam locations.

When we place the two axes of the planar array at an angle instead of orthogonal, we form a triangular array. Figure 3-16 gives the positions of a hexagon array made with equilateral triangles. We derive the characteristics of this array from a linear transformation of the rectangular array [6, p. 11-23ff]. Because the array has six-way symmetry, Figure 3-17 the pattern of a uniform-amplitude 61-element hexagon array shows the same six-way symmetry in the ring sidelobe around the main beam. If we collapsed the hexagonal distribution to a line in one plane, the distribution has a taper that reduces the sidelobes. The sidelobe amplitudes of the uniform hexagonal array are lower that the principal-plane sidelobes of the rectangular uniform array. Figure 3-18 plots the spherical pattern of the hexagon array when scanned to 36°. The first ring sidelobe has a distorted six-fold symmetry. Similar to the scanned rectangular array (Figure 3-14), the hexagon array moves more sidelobes into visible space in the area opposite the scanned main beam. Figure 3-14 showed a grating lobe entering visible space, but the hexagon array pattern in Figure 3-18 does not. The grating lobes of a rectangular array can be found from a linear array when it is scanned along one of the principal axes, but the hexagon array requires a more elaborate analysis. When we scan the rectangular array off the principal axes, we can no longer use the grating lobe analysis of linear arrays.

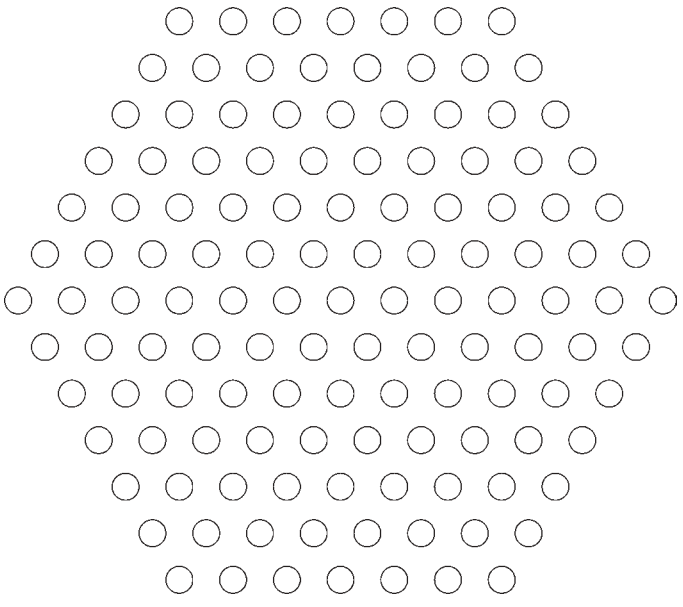

FIGURE 3-16 Position of elements in a hexagonal planar array.

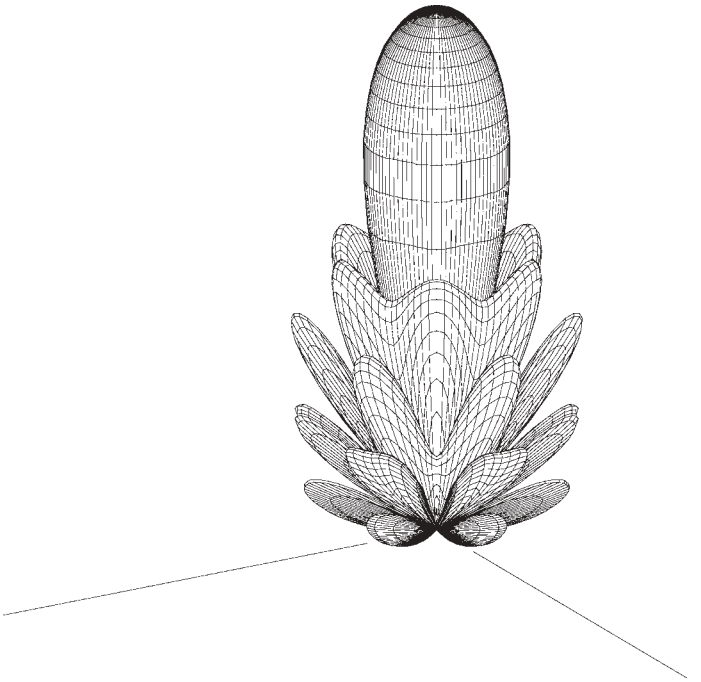

FIGURE 3-17 Spherical radiation pattern of a 61-element hexagonal array.

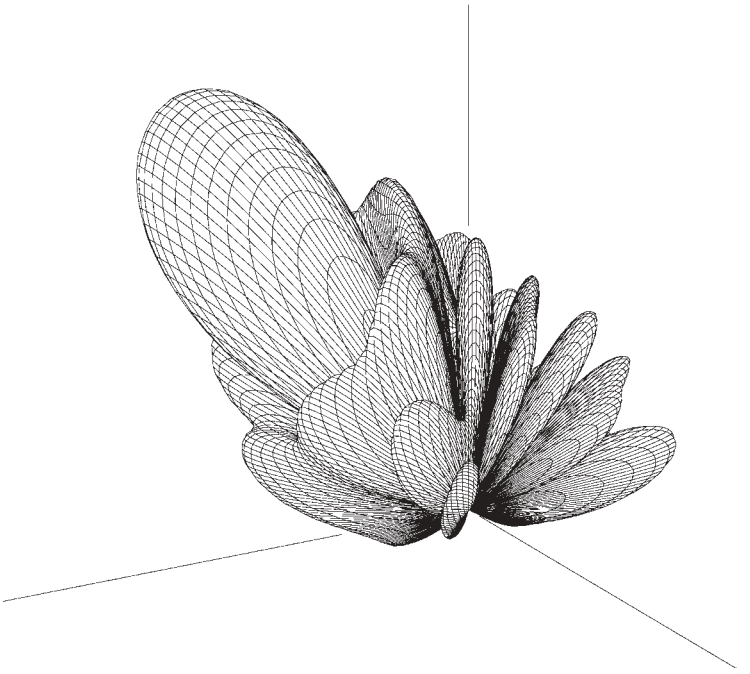

FIGURE 3-18 Spherical radiation pattern of a 61-element hexagonal array scanned along a principal plane.

3-8 GRATING LOBES IN PLANAR ARRAYS

The circle diagrams of the linear array can be used in principal planes of a rectangular array to compute grating lobes. For the planar array we use a $\sin\theta$ pattern space to see the periodicity of the grating lobes and to analyze scanning in planes other than the principal axes. The visible region is now limited to a unit circle in $k_x k_y$-space where $k_x = \sin\theta\cos\phi$ and $k_y = \sin\theta\sin\phi$. k_x is the pattern in the $x-z$ plane, and k_y is the pattern in the $y-z$ plane. Figure 3-19*a* shows the array layout, and Figure 3-19*b* shows the corresponding $k_x k_y$-plane grating lobe diagram. We reduce a contour plot of the pattern response similar to Figure 3-15 to only the main beams for analysis of grating lobes. The full contour plot is too busy. The narrower x-axis array spacing compared to the y-axis spacing leads to wider-spaced grating lobes in the k_x-plane than in the k_y-plane.

Beam scanning corresponds to movement of the unit circle in $k_x k_y$-space. Each small circle in $k_x k_y$-space is a main beam in pattern space. When the unit circle encloses more than one $k_x k_y$-circle, the pattern has multiple main beams or grating lobes. The $k_x k_y$-plane diagram could also include sidelobe peaks or the contour plot of the array pattern and illustrate the pattern change with scan. The $k_x k_y$-plane is the two-dimensional Fourier transform of the distribution that becomes the periodic two-dimensional Fourier series because the distribution is discrete. Increasing frequency or relative spacing between elements increases the unit circle diameter on an existing $k_x k_y$-diagram in a manner similar to the circle diagram.

When we scan the beam, we move the unit-circle center in $k_x k_y$-space. We use Eq. (3-13) to locate the unit-circle center on the diagram: $k(\sin\theta_0\cos\phi_0, \sin\theta_0\sin\phi_0)$. The off-center circle on Figure 3-19 corresponds to a scanned beam and encloses two main beams. In this case the grating lobe does not lie in the scan plane and would fail to show in a simple pattern cut through the scan plane. A rectangular array produces a rectangular grating lobe diagram, while other periodic arrays lead to more complicated grating lobe diagrams.

Figure 3-20 shows the layout of the hexagonal array and the corresponding grating lobe diagram. The hexagonal array (or equilateral triangular array) can be found from a linear transformation of the rectangular array. The grating lobe diagram can be found from the transformation as well. The spacing along the x-axis A_1 corresponds to the

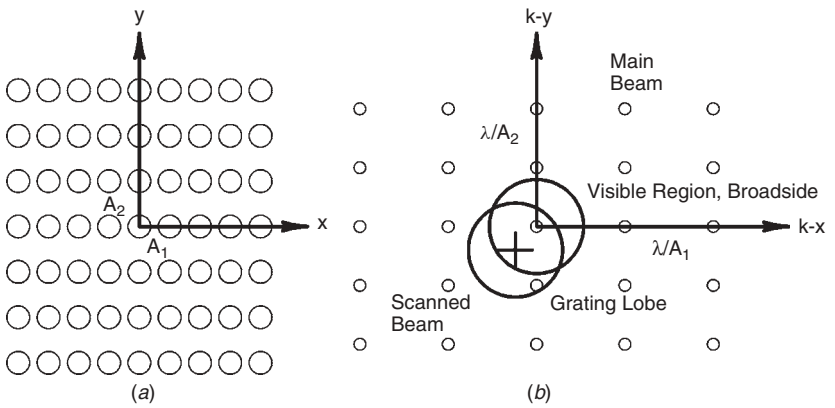

FIGURE 3-19 (*a*) Grating lobe diagram of a rectangular array; (*b*) distribution in k-space.

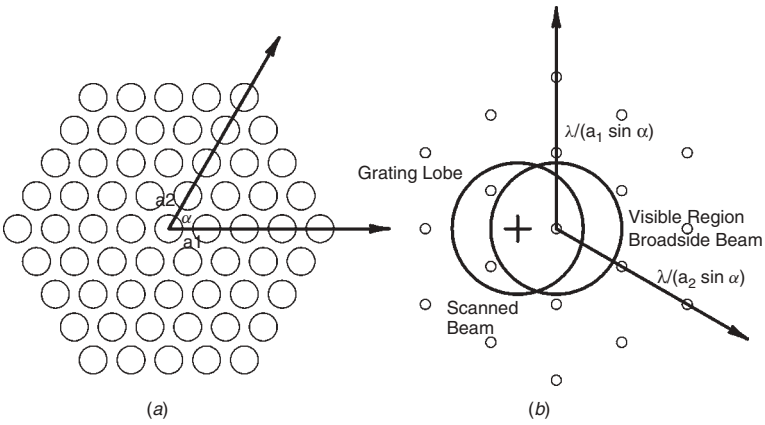

FIGURE 3-20 (*a*) Grating lobe diagram of a hexagonal array; (*b*) distribution diagram.

vertical spacing B_2 on the grating lobe diagram, and the spacing along the diagonal of each diagram are related. In both cases the corresponding axes on the two diagrams are perpendicular:

$$B_2 = \frac{\lambda}{A_1 \sin \alpha} \quad \text{and} \quad B_1 = \frac{\lambda}{A_2 \sin \alpha}$$

The angle between the triangular axes α is 60° for the hexagonal array. By allowing a grating lobe when the beam is scanned to 90°, we can determine the maximum element spacing without grating lobes:

$$\frac{\lambda}{A_1 \sin 60^\circ} = 2 \quad \text{or} \quad \frac{A_1}{\lambda} = \frac{1}{2 \sin 60^\circ} = 0.577$$

Figure 3-20 shows the visible region unit circle with the beam broadside to the plane and then scanned to 36° for an element spacing of λ. When scanned, the unit circle encloses three lobes. The three lobes do not lie in a plane. Figure 3-21 gives the

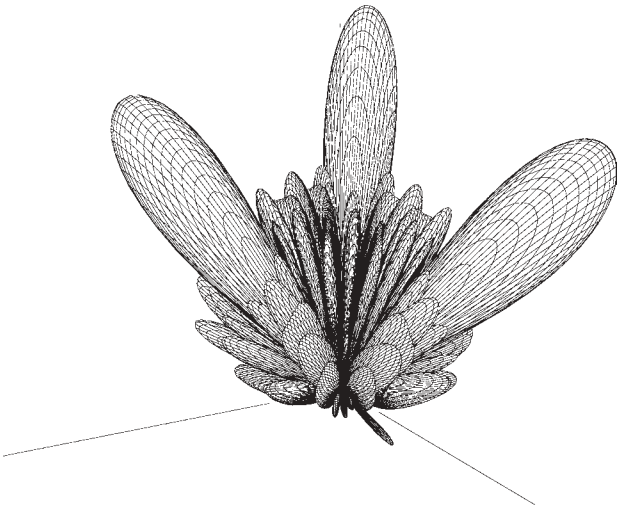

FIGURE 3-21 Spherical radiation pattern of hexagon-array grating lobes.

spherical pattern of the array when scanned to 36° and shows the three lobes in the pattern. The array sidelobes have been reduced by sampling a circular Taylor distribution with the array so that the lobes show clearly. In Chapter 4 we discuss the use of continuous aperture distributions to determine the feed amplitudes of planar arrays.

3-9 MUTUAL IMPEDANCE

Antennas in an array couple to each other because they receive a portion of the power radiated from nearby elements. This affects the input impedance seen by each element, which depends on the array excitation. We scan a phased array by changing the feeding coefficients, and this changes the element input impedance called the *scan impedance*. To first order, the coupling or mutual impedance is proportional to the element pattern level along the array face, and we reduce coupling by using narrower-beamwidth elements. Mutual coupling can be represented by an impedance, admittance, or scattering parameter matrix.

The first element of an N-element array has the impedance equation

$$V_1 = Z_{11}I_1 + Z_{12}I_2 + Z_{13}I_3 + \cdots + Z_{1N}I_N$$

If we know the radiation amplitudes, we calculate the ratio of the currents:

$$V_1 = I_1\left(Z_{11} + \frac{I_2}{I_1}Z_{12} + \frac{I_3}{I_1}Z_{13} + \cdots + \frac{I_N}{I_1}Z_{1N}\right)$$

The effective or scan impedance of the first element is

$$Z_1 = \frac{V_1}{I_1} = Z_{11} + \frac{I_2}{I_1}Z_{12} + \frac{I_3}{I_1}Z_{13} + \cdots + \frac{I_N}{I_1}Z_{1N} \tag{3-18}$$

It depends on the self-impedance and the excitation of all the other antennas. *Scan impedance* was formerly called *active impedance*, but this led to confusion. The power into the first element is

$$P_1 = \mathrm{Re}(V_1 I_1^*) = I_1 I_1^* \mathrm{Re}\left(Z_{11} + \frac{I_2}{I_1}Z_{12} + \frac{I_3}{I_1}Z_{13} + \cdots + \frac{I_N}{I_1}Z_{1N}\right) \tag{3-19}$$

By knowing the feeding coefficients and the mutual impedances, we can compute the total input power and gain. In general, every antenna in the array has different input impedances. As the feeding coefficients change in a phased array to scan the beam, so will the impedance of elements. The scan impedance change with scan angle causes problems with the feed network. We can repeat the same arguments for slots using mutual conductance, since magnetic currents are proportional to the voltage across each slot.

3-10 SCAN BLINDNESS AND ARRAY ELEMENT PATTERN [7, pp. 339–355; 8, pp. 365–366]

Large arrays made from elements with wide beamwidths can exhibit scan blindness. When a phased array is scanned, at certain angles the input reflection coefficient of every element rapidly increases to 1. The array fails to radiate and forms a pattern

null. Mutual coupling between elements causes the change of the scan impedance, which leads to scan blindness, which is complicated and difficult to predict accurately except where the array structure supports a surface wave. One approach says that scan blindness occurs when a grating lobe first enters from invisible space and radiates along the surface of the array. In this case we solve Eq. (3-16) for the scan angle of the grating lobe:

$$|\cos\theta_{\text{gr}}| = \frac{\lambda}{d} - 1 \tag{3-20}$$

The angle in Eq. (3-20) is measured from the array plane (or axis). Scan blindness occurs approximately at this angle, but it can be reduced to only a dip in the pattern if the array is small or the mutual coupling between the elements is small, because they have narrow beams.

The grating lobe causes a large increase in mutual coupling. Arrays made with antennas that can support surface waves, such as microstrip patches on dielectric substrates, can exhibit scan blindness when the electrical distance between the elements equals the surface-wave propagation phase shift:

$$|\cos\theta_{\text{gr}}| = \frac{\lambda}{d} - \frac{k_{\text{sw}}}{k} = \frac{\lambda}{d} - P \tag{3-21}$$

P is the relative propagation constant with a value > 1 for a surface wave (Section 10-1). Scan blindness will occur at an angle near this value because of the complicated nature of the coupling addition in the array.

We can build a small portion of the array and determine where scan blindness will occur. Feed the center element and load all others with the feeder resistance. Each element in an array will couple to its neighboring elements and we can associate the combination of the element radiation and the coupled radiation of the neighbors when loaded to the element. We call this the *array element pattern* or *scan element pattern* (formerly called the *active pattern*). Elements near the edges will have different effective patterns, but in a first-order solution we assume the pattern of the center element for all and calculate the total pattern as the product of the element pattern and the array factor. The array element pattern will exhibit dips where scan blindness will occur in the full array. Because it is only a small portion of the array, the full scan blindness will not occur. You should build a small array and test for scan blindness whenever it is a possibility. For example, arrays that scan to large angles off broadside using broad-beamwidth elements need to be tested with a small array before building the complete array.

3-11 COMPENSATING ARRAY FEEDING FOR MUTUAL COUPLING

Mutual coupling (impedance) is a measure of how much one antenna receives radiation from its neighbors in the array. Each element radiation changes the effective excitation on its neighbors. In a large array not requiring exact patterns, the effects average out. But when the array is small or you try to achieve low sidelobes, mutual coupling must be compensated for in the array. Small antenna elements such as dipoles or slots are resonant structures that radiate in only one mode. Mutual coupling only changes the element excitation, not the shape of the current distribution on the element. In this case we measure or calculate the mutual coupling matrix and use it to compute element

excitation to achieve the desired excitation [9]. Find the coupling matrix by adding the identity matrix to the S-parameter matrix of the antenna coupling:

$$\mathbf{C} = \mathbf{I} + \mathbf{S} \tag{3-22}$$

We compute the new feed excitation from the desired excitation and matrix inverse of Eq. (3-22):

$$\mathbf{V}_{\text{required}} = \mathbf{C}^{-1}\mathbf{V}_{\text{desired}} \tag{3-23}$$

Because we assumed a single mode distribution on the antenna elements, **S** is independent of scanning and Eq. (3-23) gives the compensation for all scan angles. The compensation can be applied to the received signal in an adaptive array by matrix multiplication in digital signal processing. The effects of these operations have been illustrated [10]. Without compensation adaptive arrays, such as the MUSIC algorithm, only generate small peaks, whereas compensation produces the expected large peaks.

Compensation for multimode elements starts with a moment solution [11] and uses the pattern characteristics to solve for the feeding coefficients. We use the pattern desired to compensate the feeding coefficients. We start with a matrix between the pattern response and the currents on all the antenna elements found from a moment method solution, where each array element has multiple current segments:

$$\mathbf{A}(\mathbf{k}) = \mathbf{FI} \tag{3-24}$$

$\mathbf{A}(\mathbf{k}_i)$ is an element of the column matrix that gives the pattern response at an angle given by $\mathbf{k}_i = \hat{\mathbf{x}}\sin\theta_i\cos\phi_i + \hat{\mathbf{y}}\sin\theta_i\sin\phi_i + \hat{\mathbf{z}}\cos\theta_i$ or a given pattern angle (θ_i, ϕ_i). The elements of the matrix **F** are the isotropic element phase terms, $e^{j\mathbf{k}_i\cdot\mathbf{r}_j}$, and **I** is the column vector of the currents on the segments. We calculate excitation voltages by inverting the mutual impedance matrix:

$$\mathbf{I} = \mathbf{Z}^{-1}\mathbf{V} \tag{3-25}$$

We substitute Eq. (3-25) into Eq. (3-24) and note that the matrix **V** has only q nonzero terms corresponding to the feed points. We specify q pattern points, which reduces **F** to $q \times M$ for M current segments. The vector **V** has $M - q$ zero elements and we delete the corresponding columns in the matrix product $\mathbf{FZ}^{-1}$. This reduces the matrix to $q \times q$, denoted **B:**

$$\mathbf{A}(\mathbf{k}) = \mathbf{BV}'$$

This uses the nonzero element $\mathbf{V}'$. We solve for the feeding coefficients by inverting the matrix **B** found from q pattern points:

$$\mathbf{V}' = \mathbf{B}^{-1}\mathbf{A}(\mathbf{k}) \tag{3-26}$$

Choosing good pattern points is an art that requires pattern evaluation to verify whether the final pattern is acceptable.

3-12 ARRAY GAIN

We can use the mutual impedance concept to determine the effective input power of every element and thereby avoid having to integrate the pattern to calculate average

radiation intensity. We represent the circuit relations of two antennas by a two-port impedance matrix:

$$\begin{bmatrix} V_1 \\ V_2 \end{bmatrix} = \begin{bmatrix} Z_{11} & Z_{12} \\ Z_{21} & Z_{22} \end{bmatrix} \begin{bmatrix} I_1 \\ I_2 \end{bmatrix}$$

Symmetrical elements across the diagonal of the matrix are equal for antennas satisfying reciprocity. The total input power is given by

$$P_{\text{in}} = \text{Re}(V_1 I_1^*) + \text{Re}(V_2 I_2^*)$$

The general N-element array has an $N \times N$ matrix and N terms in the input power sum. Given the feed coefficients, we have a relation between different I_i. For our two elements,

$$I_2 = I_1 e^{j\delta} \quad \text{and} \quad V_1 = (Z_{11} + Z_{12} e^{j\delta}) I_1$$

The power into the first element is

$$\text{Re}(Z_{11} + Z_{12} e^{j\delta}) I_1 I_1^*$$

By symmetry, the power into the second antenna is the same. The total input power to the array is

$$P_{\text{in}} = 2\ \text{Re}(Z_{11}) I_1 I_1^* \left[1 + \frac{\text{Re}(Z_{12} e^{j\delta})}{\text{Re}(Z_{11})} \right]$$

The factor $\text{Re}(Z_{11}) I_1 I_1^*$ is the power into an isolated element: $4\pi E_0^2/\eta$. The average radiation intensity (100% efficient antenna) is $P_{\text{in}}/4\pi$:

$$\text{gain} = \text{directivity} = \frac{|2E(\theta_{\max})|^2/\eta}{P_{\text{in}}/4\pi} = \frac{|2E(\theta_{\max})|^2}{1 + [\text{Re}(Z_{12} e^{j\delta})]/[\text{Re}(Z_{11})]} \tag{3-27}$$

By comparing Eqs. (3-27) and (3-8), we can identify

$$\frac{\text{Re}(Z_{12} e^{j\delta})}{\text{Re}(Z_{11})} = \frac{R_{12} \cos\delta}{R_{11}} = \frac{\sin(2\pi d/\lambda) \cos\delta}{2\pi d/\lambda}$$

$$\frac{R_{12}(d)}{R_{11}} = \frac{\sin(2\pi d/\lambda)}{2\pi d/\lambda}$$

We can use this mutual impedance ratio to compute directivity of arrays of isotropic elements of any number.

Example Calculate the directivity of a linear array of three equally spaced isotropic elements with equal amplitudes and phases.

The powers into the elements are

$$P_1 = P_3 = \frac{4\pi E_0^2}{\eta} \left[1 + \frac{R_{12}(d)}{R_{11}} + \frac{R_{12}(2d)}{R_{11}} \right]$$

$$P_2 = \frac{4\pi E_0^2}{\eta} \left[1 + \frac{2R_{12}(d)}{R_{11}} \right] \qquad U_{\max} = \frac{3^2 E_0^2}{\eta}$$

The total power into the array is found from the sum:

$$P_t = P_1 + P_2 + P_3 = \frac{4\pi E_0^2}{\eta}\left[1 + \frac{4R_{12}(d)}{R_{11}} + \frac{2R_{12}(2d)}{R_{11}}\right]$$

$$\text{directivity} = \frac{U_{\max}}{P_t/4\pi} = \frac{9}{3 + [4R_{12}(d)/R_{11}] + [2R_{12}(2d)/R_{11}]}$$

The directivity of the general N-element equally spaced linear array, excited by equal-amplitude and equal-phase signals, is easily found by extending the development:

$$\text{directivity} = \frac{N^2(\text{element directivity})}{N + 2\sum_{M=1}^{N-1}(N-M)[R_{12}(Md)/R_{11}]} \tag{3-28}$$

The directivity attained in an array depends on the particular mutual impedance terms of the radiators. The equation above only handles uniform-amplitude linear arrays. We can extend the idea of mutual resistance to calculate input power to a general planar array consisting of identical elements and determine gain.

By using a two-element array spaced along the x-axis we can integrate the pattern to compute directivity and from that determine the ratio of mutual resistance to self-resistance of the elements versus element spacing:

$$\frac{R_{12}(x)}{R_{11}} = \frac{\text{element directivity}}{2\pi}\int_0^{2\pi}\int_0^{\pi} E_e^2(\theta,\phi)\cos^2\left(\frac{\pi x}{\lambda}\cos\phi\sin\theta\right)\sin\theta\, d\theta\, d\phi - 1 \tag{3-29}$$

Equation (3-29) uses the normalized element pattern in the integral. By using an axisymmetrical element pattern, we calculate the ratio of resistances at a number of different distances and interpolate on the table for the directivity (gain) analysis of a planar (linear) array. If the element pattern is not symmetrical, the normalized resistance must be calculated for a number of ϕ. Given the element excitations E_i with elements located at the vector locations $\boldsymbol{x}_i$, we can derive an equation similar to Eq. (3-28) for directivity of a planar array:

$$\text{directivity} = \frac{\left|\sum_{i=1}^{N} E_i\right|^2 (\text{element directivity})}{\sum_{i=1}^{N}\sum_{j=1}^{N}[R_{12}(|\mathbf{x}_i - \mathbf{x}_j|)/R_{11}]\text{Re}[E_j/E_i]|E_i|^2} \tag{3-30}$$

Figure 3-22 illustrates the directivity calculated from Eq. (3-30) for linear arrays with realistic elements, such as a microstrip patch with 90° beamwidths, as the element spacing is varied. The graph shows directivity reduction when the element spacing exceeds λ and grating lobes form a more pronounced characteristic as the number of elements increases. When the second grating lobe occurs for wider element spacing, the directivity exhibits only minor variations. Increasing the element directivity (decreased beamwidth) reduces variation because the element pattern reduces the grating lobe.

We use Eq. (3-30) with a planar array to obtain Figure 3-23. This array consists of 217 elements arranged in a hexagonal pattern, with amplitudes found from sampling a circular Taylor distribution (Sections 4-18 and 4-19) to lower the sidelobes. The 30-dB circular Taylor distribution reduces the gain by 0.6 dB relative to a uniform distribution

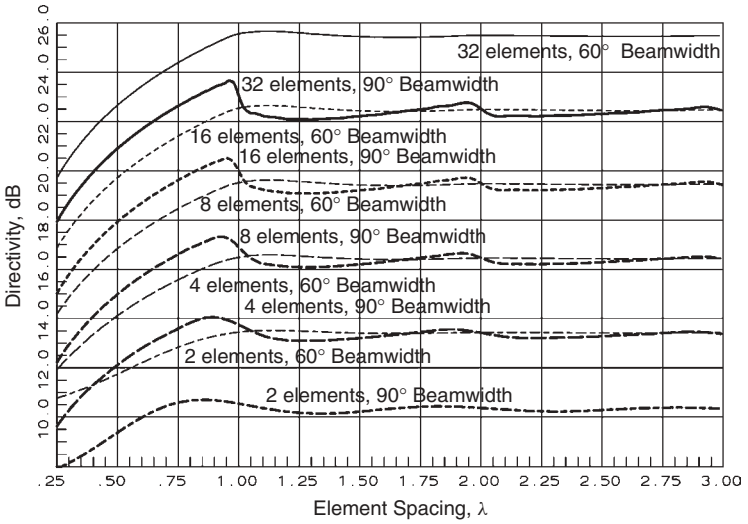

FIGURE 3-22 Directivity of a uniform-amplitude line array versus element spacing for 60° and 90° beamwidth elements.

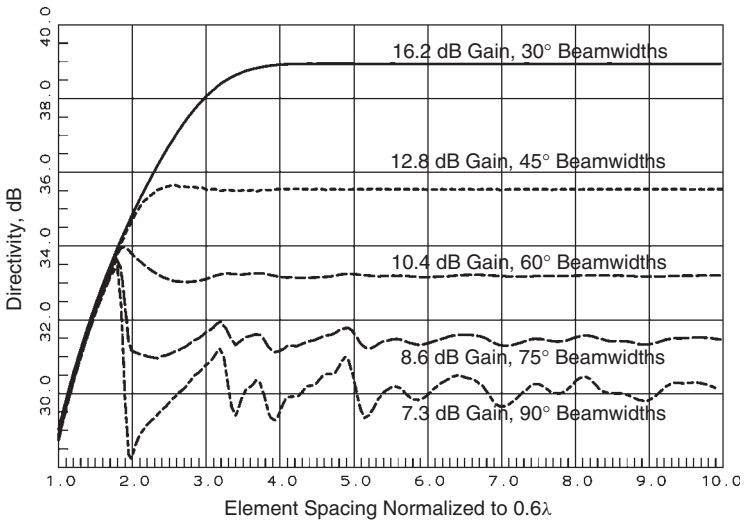

FIGURE 3-23 Directivity of a 217-element uniform-amplitude hexagonal array for various element beamwidths versus spacing.

due to the amplitude taper across the array. Initially, the element spacing is 0.6λ, but the element spacing has been allowed to grow in Figure 3-23 to show the effect. Figure 3-23 also illustrates the effect of increasing the element gain on the gain of a planar array. When we space the elements less than λ, increasing the element gain has no effect on array gain because the effective area of an antenna with a 90° beamwidth exceeds the area between elements and collects all power incident on the array. If we increase the element gain, the effective areas of the elements overlap and they share the incident power. On Figure 3-23 the curves overlap for element spacing less than

about λ. At the lower end of Figure 3-23 the gain increases by 6 dB as the element spacing doubles. This shows that increasing the element gain will have no effect on array gain when the present element covers the area associated with it.

When the grating lobe enters from invisible space as the element spacing increases, those arrays with narrower-beam elements suppress the lobes and continue the general gain increase. The array directivity (gain) drops as the element spacing increases for the wide-beamwidth element with 90° beamwidth because of the grating lobe. At a large element spacing the array gain becomes N times the element gain. We determine array gain from the array area and the amplitude taper for closely spaced elements. For wide element spacing, we calculate gain from the product of the number of elements and the element gain. Figure 3-23 shows a smooth transition between the two regions.

3-13 ARRAYS USING ARBITRARILY ORIENTED ELEMENTS

When we mount arrays on vehicles, the elements are pointed in arbitrary directions. Although Eq. (3-1) will calculate the pattern of any array, the element patterns are usually measured in a coordinate system in a different orientation than in the array. The idea of an array factor times the element pattern collapses and an analysis must rotate the pattern direction into the coordinates of each element. We will use coordinate rotations on the elements not only to specify them, but to calculate the pattern of the array. In a later chapter we use the same concept to point a feed antenna at a reflector.

We rotate the pointing direction into the coordinate system of the orientated antenna to determine what direction angles to use for the element pattern. We do this by using a 3×3 rotation matrix on rectangular components:

$$[X_{\text{rotated}} \quad Y_{\text{rotated}} \quad Z_{\text{rotated}}] = [\text{rotation matrix}] \begin{bmatrix} X \\ Y \\ Z \end{bmatrix} \tag{3-31}$$

A similar problem is rotating an object. Both cases use the same matrix. To rotate an object we multiply the vector by the rotation matrix from the left to compute the rotated coordinates. Rotating a position is given by the equation

$$[X_{\text{old}} \quad Y_{\text{old}} \quad Z_{\text{old}}][\text{rotation matrix}] = \begin{bmatrix} X_{\text{rotated}} \\ Y_{\text{rotated}} \\ Z_{\text{rotated}} \end{bmatrix} \tag{3-32}$$

The rotation matrix can be found from the directions of the unit vectors when rotated. It is given by

$$\text{rotation matrix} = \begin{bmatrix} \text{rotated } X\text{-axis} \\ \text{rotated } Y\text{-axis} \\ \text{rotated } Z\text{-axis} \end{bmatrix} \tag{3-33}$$

The method uses 3×3 matrices to perform the rotation by a multiplication with a position or direction vector. Rotation about the X-axis is given by

$$\begin{bmatrix} 1 & 0 & 0 \\ 0 & \cos A & \sin A \\ 0 & -\sin A & \cos A \end{bmatrix}$$

rotation about the Y-axis is given by

$$\begin{bmatrix} \cos B & 0 & -\sin B \\ 0 & 1 & 0 \\ \sin B & 0 & \cos B \end{bmatrix}$$

and rotation about the Z-axis is given by

$$\begin{bmatrix} \cos C & \sin C & 0 \\ -\sin C & \cos C & 0 \\ 0 & 0 & 1 \end{bmatrix}$$

We use products of these axis rotations to reorient an object or pointing direction. Consider the rotation of a position by the product of three rotation matrices:

$$[X_{\text{old}} \quad Y_{\text{old}} \quad Z_{\text{old}}]\mathbf{R}_1\mathbf{R}_2\mathbf{R}_3 = \begin{bmatrix} X_{\text{rotated}} \\ Y_{\text{rotated}} \\ Z_{\text{rotated}} \end{bmatrix}$$

The logical approach is to multiply the 3×3 matrices, $\mathbf{R}_1$, $\mathbf{R}_2$, and $\mathbf{R}_3$, before multiplying by the position vector. When we postmultiply $\mathbf{R}_1$ by $\mathbf{R}_2$, it rotates the axis of rotation of $\mathbf{R}_1$. The postmultiplication by $\mathbf{R}_3$ rotates the rotation axis $\mathbf{R}_2$ and $\mathbf{R}_1$ is rotated once more. We can take the rotations one by one from left to right and use the rotation matrices about each of the principal axes provided that we convert the column vector back to a row vector after each multiplication.

A convenient way to define the orientation of objects in space is to use spherical coordinate angles, since they are the same as pattern angles. We line up the matrices from right to left in this case. When rotating the coordinate system about an axis, the other axes change direction. The next rotations are about these new axes. The three rotations are often called the *Euler angles*. We use the following three rotations for spherical coordinate pointing:

1. Z-axis rotation $= \phi$
2. New Y-axis rotation $= \theta$
3. New Z-axis rotation: aligns the polarization of the antenna

The last rotation takes some thought because the first two rotations have altered the orientation of the antenna.

When calculating the pattern of the array for a particular direction, first compute rectangular components of the direction vector and the two polarization vectors. Multiply the direction vector by $k(2\pi/\lambda)$ and take the dot (scalar) product with the position vector to calculate phasing of a particular element. You need to determine the pattern direction in the rotated antenna's coordinate system found by using Eq. (3-31). Multiply the rotation matrix by the unit direction vector placed to the right. When you convert the output vector to spherical coordinates, you obtain pattern coordinates of the rotated antenna. Both the pattern components of the rotated element and the unit polarization vectors are needed. In the next operation you rotate the prime coordinate polarization unit vectors into the rotated element coordinate system using the same operation as the direction vector.

You calculate final radiated components by projecting the rotated prime coordinate polarization vectors on the element pattern unit polarization vectors:

$$E_\theta = E_{\theta,\text{element}}\hat{\theta}_{\text{element}} \cdot \hat{\theta}_{\text{rotated}} + E_{\phi,\text{element}}\hat{\phi}_{\text{element}} \cdot \hat{\theta}_{\text{rotated}}$$
$$E_\phi = E_{\theta,\text{element}}\hat{\theta}_{\text{element}} \cdot \hat{\phi}_{\text{rotated}} + E_{\phi,\text{element}}\hat{\phi}_{\text{element}} \cdot \hat{\phi}_{\text{rotated}} \quad (3\text{-}34)$$

Since we measure element patterns on antenna positioners, it is convenient to consider positioners as a series of coordinate system rotations.

REFERENCES

1. C. A. Balanis, *Antenna Theory, Analysis and Design*, 2nd ed., Wiley, New York, 1997.
2. W. W. Hansen and J. R. Woodyard, A new principle in directional antenna design, *Proceedings of IRE*, vol. 26, March 1938, pp. 333–345.
3. T. C. Cheston and J. Frank, Array antennas, Chapter 11 in M. I. Skolnik, ed., *Radar Handbook*, McGraw-Hill, New York, 1970.
4. J. L. Butler, Digital, matrix, and intermediate frequency scanning, Section 3 in R. C. Hansen, ed., *Microwave Scanning Antennas*, Vol. III, Academic Press, New York, 1966.
5. J. Blass, The multidirectional antenna: a new approach to stacked beams, *IRE International Convention Record*, vol. 8, pt. 1, 1960, pp. 48–50.
6. Y. T. Lo and S. W. Lee, eds., *Antenna Handbook*, Vol. II, Van Nostrand Reinhold, New York, 1993.
7. R. J. Mailloux, *Phased Array Antenna Handbook*, Artech House, Boston, 1994.
8. P.-S. Kildal, *Foundations of Antennas*, Studentlitteratur, Lund, Sweden, 2000.
9. H. Steyskal and J. S. Herd, Mutual coupling compensation in small array antennas, *IEEE Transactions on Antennas and Propagation*, vol. AP-38, no. 12, December 1990, pp. 1971–1975.
10. A. G. Derneryd, Compensation of mutual coupling effects in array antennas, *IEEE Antennas and Propagation Symposium*, 1996, pp. 1122–1125.
11. B. J. Strait and K. Hirasawa, Array design for a specified pattern by matrix methods, *IEEE Transactions on Antennas and Propagation*, vol. AP-18, no. 1, January 1971, pp. 237–239.